Vietnam Journal of Catalysis and Adsorption
Tạp chí xúc tác và hấp phụ Việt Nam

http://jca.edu.vn

Large-scale synthesis of reduced-graphene oxide and its applications in supercapacitors

Le Minh Tri[1,*], Nguyen Huu Van[2,*]

[1] *Academy of Military Science and Technology, Nghia Do, Cau Giay, Ha Noi, VIET NAM*
[2] *Institute of Chemistry and Materials Science, Nghia Do, Cau Giay, Ha Noi, VIET NAM*
**Email: leminhtri19751977@gmail.com, vanhd2@gmail.com,*

ARTICLE INFO

Received: 18/06/2024
Accepted: 22/09/2024
Published: 30/09/2024

Keywords:
Reduced Graphene oxide; electrochemical exfoliation; supercapacitors; EDLCs.

ABSTRACT

Graphene-based electrode materials exhibit a high specific capacitance and long charge-discharge cycling life, but the material cost remains high because of the complexity of the graphene manufacturing process. This study employed an electrochemical exfoliation method to prepare graphene in a simple and ecologically friendly procedure. According to research findings, the disordered multi-layer structure of graphene exhibited great purity, porosity, and graphitization. The graphene electrode material showed high electrochemical properties in a two-electrode supercapacitor system, with a specific capacitance of 168.2 F g^{-1} at a current density of 0.1 A g^{-1} and a specific capacitance retention of 94.5 % after 1000 cycles. Research shows enormous potential of electrochemical approaches for producing large-scale graphene materials for energy storage application.

1. Introduction

Graphene is one atom thick in layer of carbon, tightly bound in a hexagonal honeycomb lattice. The substantial π-electron conjugation in graphene results in fascinating electronic, thermal, magnetic, optical, mechanical, and chemical properties [1-3]. Because of outstanding properties, graphene finds prominent applications in the electronic devices such as supercapacitor [4]; battery [5]; solar cell [6] and sensors [7]. In addition, other essential applications are printed electronics, conductive coatings [8] and energy storage [9], etc. The most widely used derivative of graphene, graphene oxide (GO), is a chemically changed graphene material with many functionalities containing O on its planes and edges, especially having low C/O ratio.

In the last decade, there were many methods have been explored for the production of graphene, which can be broadly categorized into two groups [10]. The first method group is the bottom-up method, by which the graphene sheets can be grown from individual molecules, including organic solvent, chemical vapor deposition of gaseous carbon precursors on solid catalytic substrate [11-13]. The second method group is the top-down method. Since the graphene can be considered as the core structural form of graphite, carbon nanotubes (CNTs) and many other kind of carbonaceous nanomaterials so that it is impossible to get graphene materials via the exfoliation of those by mechanical, chemical, thermal or electric route [14,15]. Different fabrication methods can produce graphene with variety of shapes, qualities and sizes. The most widely used derivative of graphene, graphene oxide (GO), is a chemically modified graphene material with numerous functionalities containing O on its planes and edges, especially having low C/O ratio. The reduced graphene oxide (rGO) involves three steps: the preparation of GO with the support of chemical exfoliation, the exfoliation of GO, and the reduction of GO [16]. With relatively milder mechanical forces, GO can be exfoliated from graphite and stabilized in various

https://doi.org/10.62239/jca.2024.060

solvents owing to repelling forces among GO sheets introduced by their surfacer functional groups [17].

However, synthesizing graphene often faces a critical tradeoff between the yield and properties of the resulting graphene material. For instance, mechanical exfoliation of graphite without chemical fractionalization has low production yield and the reduction of graphene oxide can produce rGO at higher yield, which leads to the commercialized technique. Although many reduction procedures can produce GO, they still cannot meet the properties of graphene [18].

Because of the limited scalability and relatively high production cost, the methods such as mechanical exfoliation, synthesis on SiC with bottom-up procedure from structurally defined organic precursors restrict the use of graphene to fundamental research and practical applications. Similar with chemical vapor deposition (CVD) of hydrocarbon, although it is well-known as a well-established technique in industry, but it seems unsuitable for mass production of graphene for energy storage applications because of its high cost and low yield of production as well. However, CVD has been reported as an efficient method for producing vertically oriented graphene nano sheets electrode [19] even though the density of obtained graphene is extremely low. Moreover, two methods which are widely applied for the bulk production of graphene are liquid-phase exfoliation and reduction of graphene oxide. In the liquid-phase exfoliation process, pristine or expanded graphite particles are first immersed in a solvent to reduce the strength of Van der Waals attraction among graphene layers. Thereafter, an external driving force, such as electric field [20] or shearing [21], is used to stimulate the exfoliation of graphite into well-defined graphene sheets [10]. Unfortunately, it remains some problems, the low yield of this process leaves a significant amount of unexfoliated graphite that must be removed. However, the scalability and low-cost of this method make it suitable for producing graphene in bulk quantity. In the second method, GO, a highly defective form of graphene, with a disrupted sp^2-bonding network, is produced by strong oxidation of pristine graphite followed by stirring or ultra-sonication in liquid media [22]. GO must be reduced in order to restore the Π network, which is the characteristic of conductive graphene. Chemical, thermal or electrochemical processes are commonly employed to produce rGO from GO [23]. Despite the low-quality of obtained material because of the presence of both intrinsic defects (edges and deformations) and extrinsic defects (O- and H- containing groups), these methods still allow for the production of bulk qualities with high yield and relatively low costs.

In recent years, electrochemical exfoliation of graphite has become a simple method for producing graphene material [24]. As illustrated in Fig. 2, graphite in a variety of geometries, such as powders, foils, rods, flakes or plate, can be used as a working electrode in the liquid electrolytes [25]. The resulting graphene of different defect densities, O contents, numbers of layers, and lateral sizes can be obtained by controlling the progress parameters such as applied potentials, current density, processing time and the properties of electrolyte.

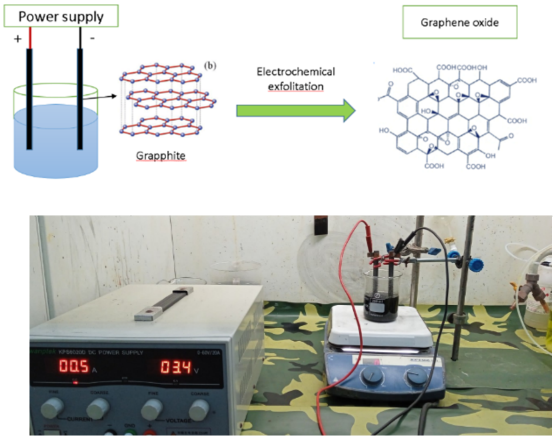

Fig 1. Schematic illustration of Graphene oxide

Over the past few years, many studies have explored based materials for energy storage applications [26]. To solve the environmental issues and depletion of fossil fuels, researchers have paid attention to the development of alternative energy storage and conversion devices. Electrochemical supercapacitors are such attractive devices owing to their high power performance, long cycle life, broad range of operation condition, and high rate of charge-discharge [27]. Supercapacitors (SCs) exploit super-fast charge storage mechanisms to enable considerably higher power densities than those available in Lithium-ion batteries (LIBs) and Sodium-ion batteries (SIBs).

Based on charge storage mechanisms, supercapacitors are classified into two types: (i) electrochemical double layers capacitors (EDLC) that store energy non Faradically via the accumulation of charge at the electrode-electrolyte interface and (ii) redox capacitors that store energy Faradically by battery-like oxidation-reduction reactions leading to pseudo-capacitive behaviors [27]. The electrode materials of EDLC commonly are mainly porous carbon materials such as graphene, activated carbon, carbon aerogels, mesoporous carbon, carbon nanotubes,… [28].

Graphene can be considered as an active material when it engages in the energy storage mechanism. This might range from hosting ions (such as Li^+ in LIBs and Na^+ in SIBs) to store electrostatic charges on the electrode double layers in EDLCs.

As mentioned above, graphene can be prepared at a large scale by reducing GO, which can be produced via electrochemical exfoliation in aqueous media. Some reducing methods have been developed, including thermal reduction or chemical reduction with reducing agents, such as sodium borohydride or hydrazine hydrate. Compared to others, the thermal reduction method can produce fewer layer graphene with less agglomeration, higher specific surface area, and higher electrical conductivity [29]. In this paper, graphene was obtained by reducing GO from electrochemical exfoliation. The thermal reduction and microwave-assisted reduction are employed in order to obtain graphene.

2. Experimental

Material

H_2SO_4, KOH were commercially available from Fisher Scientific. Carboxymethylcellulose (CMC), Styrene-Butadiene Rubber (SBR), black carbon Super P, and Monolayer polypropylene membranes (CELGARD 2500) were purchased from TMAX, China.

Graphite electrodes, Titanium electrodes were commercially available from Chinese suppliers.

Preparation of GO

The synthesis of GO contains two sequential electrochemical (EC) processes at ambient temperature with commercial flexible graphite paper (FGP) as raw material and also the working electrode (anode). The experiment setup is shown in Fig. 1. The commercial FGP has a similar structure to graphite, thus it possesses excellent electrical conductivity and excellent adaptability. It has a wide range of dimension (width, thickness, length). Two models that we can use in the electrochemical exfoliation of graphite are CC (constant current) and CV (constant voltage). In this study, we use the CC method. In our experiment, six of graphite electrodes were prepared with the dimensions of 240 x 20 x 2 mm (L x W x H). A Rubidium-coated Titanium mesh was used as cathode. The experimental system, which included six graphite electrodes and a cathode, is shown in Fig. 1. H_2SO_4 acid solutions were used as the electrolyte of the electrochemical system.

Synthesis of electrochemical graphene oxide (EGO) consists of two independent stages. The first stage is the process of electrochemical intercalation of concentrated sulfuric acid into the structure of graphite clusters of the working electrodes. The first step was performed in 15 minutes at the current of 7.7 A. During this stage, all the electrodes were immersed in H_2SO_4 98%. The second stage, called oxidative exfoliation, is a process of fast destruction of the electrodes taking place at a high anodic current of 18 A in diluted H_2SO_4 50%. During this second step, it is imperative to ensure that all the electrodes are immersed in the electrolyte. After two hours, the GO was obtained by washing the GO suspension with distilled water several times.

Synthesis of rGO

GO sheets (1 g) were thermally reduced in an argon filled horizontal tube furnace with the heating rate of 5 ^oC min^{-1}. The annealing temperature was performed at 800 ^oC for an hour.

Characterization of rGO

The morphologies and structural properties of the prepared materials were characterized by Field Emission Scanning Electron Microscope (FESEM; HITACHI S-4800) and High-resolution Transmission Electron Microscope (HRTEM; JEM 2100).

The graphitization degree was determined by a Laser Micro Raman spectrometer (Raman Microscope–DXR3, Thermo Scientific). The device uses a He-Ne laser light source, with a backscatter configuration. The sample was excited with light of wavelength 532.0 nm of the Ar laser. The crystal structure of the obtained samples was determined on an X-ray diffractometer (XRD, Bruker Advance 8).

Electrochemical measurements

To examine the electrochemical performance as supercapacitor electrodes made from prepared rGO samples, electrochemical measurements are conducted with the two-electrode configurations. Firstly, electrodes for supercapacitor were fabricated according to the optimized methods as following: the supercapacitor electrodes were made from prepared rGO, conductive agent (black carbon Super-P), and the binder: Carboxymethylcellulose (CMC). Prior to the electrode preparation, CMC was added to the SBR (CMC/SBR/DI water = 1:1:10 w/w/w). Subsequently, the rGO and carbon Super-P were added to the above solution with a rGO : carbon Super-P : CMC weight ratio of 8:1:1. After milling by the a ball milling machine for 1 hours, the mixture was coated onto a round copper foil with the diameter of 8 mm. The prepared electrodes were then dried at 60 ^oC in ambient air for 6 hours to completely

https://doi.org/10.62239/jca.2024.060

remove water content and stabilized the composite electrodes' structure. Two symmetrical electrodes were then assembled in a PTFE swagelock cell to make a two-electrode system. A monolayer polypropylene membrane (CELGARD 2500) was used as a separator, which was dipped in an aqueous solution of 6M KOH as the electrolyte.

Cyclic Voltammetry (CV) measurements, Galvanostatic Charging - Discharging (GCD) measurements and Electrochemical Impedance Spectroscopy (EIS) measurement were performed using an Autolab PGSTAT309n potentiostat (Metrohm, Switzerland).

3. Results and discussion

Morphology characterizations

The successful formation of GO and rGO with the method illustrated in Fig. 1 is well confirmed by XRD measurement as shown in Fig.2a.

As seen in Fig.2a, the XRD pattern of graphite flake exhibits a strong and sharp peak (0 0 2) at 2θ = 26.5° and it disappears after the oxidation.

For GO samples, a typical (0 0 1) peak at about 11.3° is observed, exhibiting similar crystalline structure that has been previously reported [27]. On the other hand, the oxygen-containing functional groups in GO could not be completely eliminated through the thermal reduction method. A broad peak of graphite (002) at approximately 24.5° still remained in the XRD pattern of rGO nanosheets. In general, the diffraction peak of graphite flakes is very strong and sharp, while the diffraction peak of rGO is relatively weak and blunt, indicating their ultra-thin sheets.

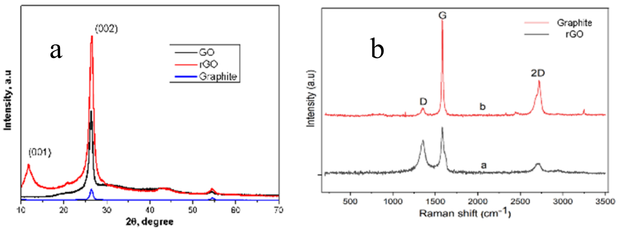

Fig 2. XRD pattern of Graphite, GO and rGO (a); Raman Spectroscopy of Graphite and rGO (b)

The Raman spectra of graphite and rGO observed in Fig.2b show peak D at ~1362 cm^{-1} and peak G at ~1600 cm^{-1}, which are the characteristic peaks of rGO material. Whereas peak 2D is indicative of the double resonance Raman scattering process, signifying the dispersion of photons and electrons in the graphene lattice, peak G represents the ordered structure of the graphite lattice, and peak D indicates the degree of defects or disordered structure of graphene oxide. The Raman spectra reveal that the peak G shift in graphene oxide (rGO) occurs at a higher frequency at 1594 cm^{-1} compared to graphite (1580 cm^{-1}), which is explained by the fact that oxidation of graphite reduces the average size of C-sp^2 graphene fragments. Following the oxidation process, there was a noticeable change and reduction in the intensity of the G and 2D peaks, with the rGO sample exhibiting a particularly sharp drop at the 2D peak position when compared to the original graphite material. It is thought that this is the result of the oxidation process, which involves increasing the number of C-sp^3 bonds relative to C-sp^2 bonds, by attaching polar functional groups to the rGO surface from the initial π bonds in the graphite network. The degree of structural change in graphene can be assessed using the ID/IG ratio. Results from the experiment indicate that functional groups and defects have been formed on the surface of the synthesized rGO sample as a result of the graphite oxidation process, with a relative intensity ratio of 0.08 for the graphite material and 0.71 for the rGO. This finding provides more evidence that graphene oxide has been produced by delamination of graphite sheets. It has been successfully fabricated with a layered structure of rGO, according to the Raman spectrum results and surface morphology images of the material, which will be discuss in following section. The graphene oxide material that was obtained has a multilayer structure with approximately 5 to 10 layers, as indicated by the ratio $I_{2D}/I_G = 0.24 < 0.4$. [30]

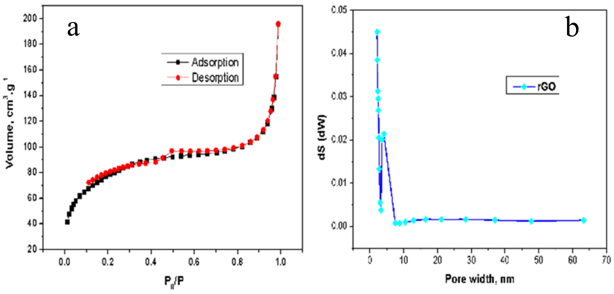

Fig 3. N_2 adsorption-desorption isotherm (a) and pore size distribution of rGO (b)

The N_2 adsorption-desorption cycle of rGO was presented in Fig. 3 show that the isotherm of material can be classified into type II model which is characteristic for macroporous materials. The adsorption of N_2 on the rGO sheets surface includes monolayer and multilayer adsorption process. The N_2 adsorption volume at the low P/P° area shows a significant overlapping of monolayer adsorption and the beginning of multilayer adsorption. The increase of adsorption volume at the

https://doi.org/10.62239/jca.2024.060

$P/P° = 1$ due to macroporous pore and multilayer N_2 diffusion and adsorption behavior. The rGO has high specific surface area $S_{BET} = 279$ m^2 g^{-1} and pore volume $V_p = 0.214$ cm^3 g^{-1}.

To examine the morphology of obtained materials, all the samples were examined by SEM and TEM, and the results are demonstrated in Fig. 4, which describes the general morphology of synthesized materials.

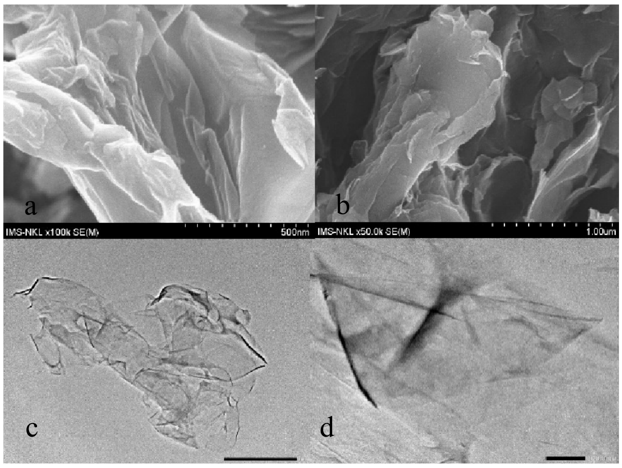

Fig 4. SEM images of rGO (a,b) and TEM images of rGO (c,d)

Fig. 4 shows that the obtained rGO has a distinct thin layer stacked on top of each other, with many wrinkles and gaps in the middle. This demonstrates that the electrochemical oxidation of a graphite electrode in H_2SO_4 acid solution produces thin-layer graphene oxide. Fig 4c,d exhibits high-resolution TEM images of the obtained rGO, highlighting the separation of layers. Fig 4c,d show the appearance of highly transparent areas on both samples, showing that the obtained rGO is a thin film made up of several layers of graphene stacked on top of each other.

Electrochemical behavior

Two electrodes of rGO – carbon Super P – CMC/SBR on copper foil and a PP membrane were assembled to fabricate the symmetric supercapacitor, which is a 2-electrode configuration. To evaluate the electrochemical performance of the supercapacitor electrode made from prepared rGO, cyclic voltammetry (CV) tests and galvanostatic charging – discharging (GCD) were carried out in a two-electrode configuration in an aqueous solution of 6 M KOH. Cyclic voltammograms at different voltage ranges as well as galvanostatic charge - discharge curves at various current densities are shown in Fig. 5.

Fig. 5a shows an almost rectangular shape of the voltammograms up to the highest voltage of 1 V, thus evidencing the absence of undesired parasitic processes in the studied ranges of voltage window. All the curves with high symmetries show that the reversibility of the electrochemical process is extremely good. The energy storage mechanism can be considered as adsorption and desorption on the surface of materials.

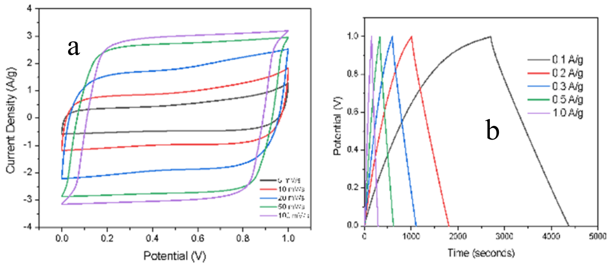

Fig 5. CV curves of supercapacitor electrodes made from prepared rGO at different scan rates (a), Galvanostatic charge/discharge curves of rGO electrodes at different current density (b)

To evaluate the specific capacitance value with two electrodes configuration, galvanic charge/discharge tests were conducted (Fig. 5b) at various current densities. According to the charge/discharge curves, the specific capacitance (C) of the obtained materials is calculated as follows [31]:

$$C = I\Delta t / m\Delta V$$

Where C is the specific capacitance of electrode (F g^{-1}), I is the discharge current density (mA cm^{-2}), t is the discharge time (s), ΔV is the potential window (V) and m is the mass of electroactive materials (mg). As shown in Fig.5b, the charging curve is nearly symmetric regarding the corresponding discharge curve in the potential range from 0 to 1 V. The specific capacitance of rGO electrode was calculated using the charge/discharge at current density of 0.1 to 1 A g^{-1}. The capacitance is high to 168.2 F g^{-1} at 0.1 A g^{-1}, 156.5 F g^{-1} at 0.2 A g^{-1}, 153.6 F g^{-1} at 0.3 A g^{-1}, 148.6 F g^{-1} at 0.5 A g^{-1} and 94.8 F g^{-1} at 1 A g^{-1}. This shows that the prepared material has excellent operating stability over a wide range of discharge current densities.

Fig 6a show the Nyquist plot of rGO electrodes. Nyquist plot of electrode samples with starting point at Z'= 0.52 Ω and 5.2 Ω of diameter semi-circle. The rGO electrode has a relatively low internal resistance R_S. The 45° inclined line representing the Warburg impedance of the rGO is short, shows that electrolyte ions can move through the rGO layers easily. Subsequently, the long-term durability assessment of symmetric supercapacitor with two electrodes on copper foil was carried out. The SC is subjected to GCD sequences. This test procedure was repeated with sets of 1000 cycles. In this way,

https://doi.org/10.62239/jca.2024.060

performing SCs is followed under stringent test conditions. The Fig 6b shows that the capacitance of supercapacitor based on rGO remains 94.5% after 1000 cycles.

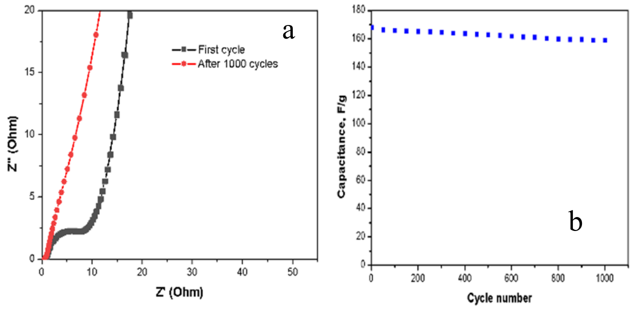

Fig 6. Nyquist plot of rGO electrode at 1st cycle and 1000th cycle (a) and Rangone plot of rGO electrode (b)

4. Conclusion

The rGO was successfully prepared by electrochemical exfoliation and simple thermal reduction method. The morphology of obtained material was characterized by SEM, TEM, XRD and used directly to fabricate electrode for supercapacitor. The obtained materials were tested for electrochemical performance with CV at a different scan rate ranging from 5 to 100 mV s^{-1} and GCD at different current densities ranging from 0.1 to 1 A g^{-1}. These structural properties contribute to the electrochemical properties of the rGO (168.2 F g^{-1} at 0.1 A g^{-1}) with high cycles stability (94.5% capacitance retention for 1000 cycles). This study provides a promising route to prepare rGO as highly efficient electrodes materials for supercapacitors.

Acknowledgments

This research is funded by the Science and Technology Development project under grant number 2023.85.37.

References

1. A.K.J.s. Geim, 324 (2009) 1530. https://doi.org/10.1126/science.1158877
2. M.J. Allen, V.C. Tung, R.B. Kaner, Chemical reviews 110 (2010) 132. https://doi.org/10.1021/cr900070d
3. R. Raccichini, A. Varzi, S. Passerini, B. Scrosati, Nature materials 14 (2015) 271. https://doi.org/10.1038/nmat4170
4. C. Liu, Z. Yu, D. Neff, A. Zhamu, B.Z. Jang, Nano letters 10 (2010) 4863. https://doi.org/10.1021/nl102661q
5. M.F. El-Kady, Y. Shao, R.B. Kaner, Nature Reviews Materials 1 (2016) 1. https://doi.org/10.1038/natrevmats.2016.33
6. S. Alex Pandian, M. Sivakumar, Materials Today: Proceedings (2023). https://doi.org/10.1016/j.matpr.2023.01.415
7. Q. Li, M. Xu, C. Jiang, S. Song, T. Li, M. Sun, W. Chen, H. Peng, Carbon 202 (2023) 561. https://doi.org/10.1016/j.carbon.2022.11.033
8. H.J. Salavagione, P.S. Shuttleworth, J.P. Fernández-Blázquez, G.J. Ellis, M.A. Gómez-Fatou, Carbon 167 (2020) 495. https://doi.org/10.1016/j.carbon.2020.05.108
9. R. Padma Priya, A. Baradeswaran, A. Bagubali, Materials Today: Proceedings (2023). https://doi.org/10.1016/j.matpr.2023.02.279
10. K.S. Novoselov, V.I. Fal' ko, L. Colombo, P.R. Gellert, M.G. Schwab, K. Kim, nature 490 (2012) 192. https://doi.org/10.1038/nature11458
11. Y. Yan, F.Z. Nashath, S. Chen, S. Manickam, S.S. Lim, H. Zhao, E. Lester, T. Wu, C.H. Pang, Nanotechnology Reviews 9 (2020) 1284. https://doi.org/10.1515/ntrev-2020-0100
12. K. Mullen, ACS nano 8 (2014) 6531. https://doi.org/10.1021/nn503283d
13. Y. Zhu, S. Murali, W. Cai, X. Li, J.W. Suk, J.R. Potts, R.S. Ruoff, Advanced materials 22 (2010) 3906. https://doi.org/10.1002/adma.201001068
14. L. Jiao, X. Wang, G. Diankov, H. Wang, H. Dai, Nature nanotechnology 5 (2010) 321. https://doi.org/10.1038/NNANO.2010.54
15. F. Liu, C. Wang, X. Sui, M.A. Riaz, M. Xu, L. Wei, Y. Chen, Carbon Energy 1 (2019) 173. https://doi.org/10.1002/cey2.14
16. D.R. Cooper, B. D'Anjou, N. Ghattamaneni, B. Harack, M. Hilke, A. Horth, N. Majlis, M. Massicotte, L. Vandsburger, E. Whiteway, International Scholarly Research Notices 2012 (2012). https://doi.org/10.5402/2012/501686
17. Y. Hernandez, V. Nicolosi, M. Lotya, F.M. Blighe, Z. Sun, S. De, I.T. McGovern, B. Holland, M. Byrne, Y.K. Gun'Ko, Nature nanotechnology 3 (2008) 563. https://doi.org/10.1038/nnano.2008.215
18. S. Pei, H.-M. Cheng, Carbon 50 (2012) 3210. https://doi.org/10.1016/j.carbon.2011.11.010
19. J.R. Miller, R. Outlaw, B. Holloway, Science 329 (2010) 1637. https://doi.org/10.1126/science.1194372
20. D. Wei, L. Grande, V. Chundi, R. White, C. Bower, P. Andrew, T. Ryhänen, Chemical communications 48 (2012) 1239. https://doi.org/10.1039/c2cc16859f
21. K.R. Paton, E. Varrla, C. Backes, R.J. Smith, U. Khan, A. O'Neill, C. Boland, M. Lotya, O.M. Istrate, P. King, Nature materials 13 (2014) 624. https://doi.org/10.1038/nmat3944
22. D. Li, M.B. Müller, S. Gilje, R.B. Kaner, G.G. Wallace, Nature nanotechnology 3 (2008) 101. https://doi.org/10.1038/nnano.2007.451
23. S. Park, R.S. Ruoff, Nature nanotechnology 4 (2009) 217. DOI: 10.1038/nnano.2009.58
24. C. Low, F. Walsh, M. Chakrabarti, M. Hashim, M. Hussain, Carbon 54 (2013)1. https://doi.org/10.1016/j.carbon.2012.11.030
25. S. Yang, M.R. Lohe, K. Müllen, X. Feng, Advanced Materials 28 (2016) 6213. https://doi.org/10.1002/adma.201505326
26. J. Hou, Y. Shao, M.W. Ellis, R.B. Moore, B. Yi, Physical Chemistry Chemical Physics 13 (2011) 15384. https://doi.org/10.1039/C1CP21915D
27. B. Zhao, P. Liu, Y. Jiang, D. Pan, H. Tao, J. Song, T. Fang, W. Xu, Journal of power sources 198 (2012) 423. https://doi.org/10.1016/j.jpowsour.2011.09.074
28. L.L. Zhang, X. Zhao, Chemical Society Reviews 38 (2009) 2520. https://doi.org/10.1039/B813846J
29. W. Bao, F. Miao, Z. Chen, H. Zhang, W. Jang, C. Dames, C.N. Lau, Nature nanotechnology 4 (2009) 562. https://doi.org/10.1038/nnano.2009.191
30. A.Y. Lee, K. Yang, N.D. Anh, C. Park, S.M. Lee, T.G. Lee, M.S. Jeong, Applied Surface Science 536 (2021) 147990. https://doi.org/10.1016/j.apsusc.2020.147990.
31. Y. Zhu, S. Murali, M.D. Stoller, A. Velamakanni, R.D. Piner, R.S. Ruoff, Carbon 48 (2010) 2118. https://doi.org/10.1126/science.1200770